

RESEARCH

Open Access



Hidden in plain sight: revisiting the synthesis, characterisation, degradation and the intricate relationship between Scheele's green and Emerald green

Leonardo Pantoja Munoz^{1*}

Abstract

Carl Wilhelm Scheele's notorious toxic pigment, commonly referred to as "Scheele's green" often resulted in a mixture of products with unknown chemical composition. Positive identification of the pigment has been limited to Raman spectroscopy and indirect analysis using FTIR and XRD methods. Despite these techniques, reported occurrences of the pigment in heritage samples are scarce, suggesting that Scheele's green is rarely reported due to challenges in its characterisation rather than infrequent use. Regarding the degradation of Cu-As green pigments, common assumptions suggest dissociation in acidic pH conditions, generating mobile arsenic and copper ions, followed by oxidation to As(V), which can co-precipitate with Fe, Al, and Ca ions. This study reproduces the fabrication of Scheele's green using historical recipes, focusing on maintaining the pH of the arsenite solution at 9.3. The research explores its relationship with Emerald green, the challenges associated with their identification, and addresses common misconceptions about the degradation of such pigments. Maintaining the pH at 9.3 proved influential in obtaining a crystalline product with an intense Raman signal, aligning with the widely accepted spectra of Scheele's green. However, Raman spectra from amorphous Cu-As samples consistently exhibited broad bands at 288 and 845 cm^{-1} , prompting a proposed modification for a dual representation of the pigment: the "common" form with broad bands and the "uncommon" or crystalline form as reported in the literature. Demonstrating that the crystalline form shares nearly identical Raman and FTIR spectra implies an identical chemical composition to Trippkeite. Evidence presented highlights that Cu-As based pigments contain free copper, arsenite and arsenate ions prone to migration, challenging commonly described degradation pathways. The hypothesis presented here, that Emerald green synthesis may inadvertently yield small amounts of Scheele's green urges caution in pigment identification using Raman spectroscopy. Additionally, the study reveals, for the first time, the occurrence of Scheele's green in a book, with particles exhibiting a spherulite form, challenging identification of Emerald green solely based on morphology.

Keywords Arsenic, Emerald green, Scheele's green, Speciation, Degradation

Introduction

History and synthesis of Scheele's green

Carl Wilhelm Scheele, a highly gifted chemist, made profound contributions to the field of chemistry, including the identification of seven elements—oxygen, chlorine, molybdenum, manganese, tungsten, barium and fluorine. Additionally, he uncovered various organic acids such as tartaric, oxalic, malic, mucic,

*Correspondence:

Leonardo Pantoja Munoz
l.pantojamunoz@mdx.ac.uk

¹ Department of Natural Sciences, Faculty of Science and Technology, Middlesex University, The Burroughs, London NW4 4BT, UK



© The Author(s) 2024. **Open Access** This article is licensed under a Creative Commons Attribution 4.0 International License, which permits use, sharing, adaptation, distribution and reproduction in any medium or format, as long as you give appropriate credit to the original author(s) and the source, provide a link to the Creative Commons licence, and indicate if changes were made. The images or other third party material in this article are included in the article's Creative Commons licence, unless indicated otherwise in a credit line to the material. If material is not included in the article's Creative Commons licence and your intended use is not permitted by statutory regulation or exceeds the permitted use, you will need to obtain permission directly from the copyright holder. To view a copy of this licence, visit <http://creativecommons.org/licenses/by/4.0/>. The Creative Commons Public Domain Dedication waiver (<http://creativecommons.org/publicdomain/zero/1.0/>) applies to the data made available in this article, unless otherwise stated in a credit line to the data.

uric, lactic, gallic and pyrogallic acids, along with the isolation of ammonia, glycerine and lactose. Scheele's pioneering work also extended to the determination of the compositions of borax and Prussian blue. Furthermore, he developed processes for pasteurisation and the production of ether, calomel, magnesia, and mass-produced phosphorus in 1769, elevating Sweden's status as a leading global producer of matches [1].

However, despite his many accomplishments, Scheele's legacy remains overshadowed by his inadvertent creation of a notorious and lethal pigment, commonly known as "Scheele's green". This pigment was rapidly welcomed by artists due to its unique vibrant hue. The pigment was used to colour fabrics, wallpaper, calico printing, window blinds, for house and ship painting as well as medicinal antiseptic, wood preservative, insecticide, fungicide and rodenticide [2]. In terms of artist materials, Scheele's green was included in the catalogue of the following companies: F. W. Devoe, Frost and Adams, Lefranc, Richard Aine and Bourgeois Aine. It is important to note that the pigment was never sold by Winsor & Newton [2, 3].

However, it was soon realised that the green pigment was unstable under certain conditions. To address the issue of Scheele's green's instability, Emerald green was specifically formulated as a direct substitute [2].

For an extended period of time, until 1822 and 1876 for Emerald and Scheele's green respectively, the manufacturing process, the exact formula and analytical characterisation were not fully understood [4, 5]. Scheele's green, while relatively straightforward to synthesise, often resulted in a mixture of products with unknown chemical composition. In contrast, the production of Emerald green posed many challenges, yet the final product was well characterised with known and accepted chemical composition [2, 6, 7].

Emerald green has been unanimously assigned the formula $3\text{Cu}(\text{AsO}_2)_2 \cdot \text{Cu}(\text{CH}_3\text{COO})_2$ [2]. In contrast, Scheele's green has been ascribed various formulas, including $2\text{CuHAsO}_3 \cdot \text{H}_2\text{O}$, $2\text{CuHAsO}_3 \cdot \text{Cu}(\text{OH})_2$ and $\text{Cu}(\text{AsO}_2)_2$, with no consensus reached to the correct one [6]. Adding to the complexity, the rare natural mineral Trippkeite shares the formula $\text{Cu}(\text{AsO}_2)_2$ [8]. This has led to speculation regarding the possibility of Trippkeite and Scheele's green sharing an identical composition, implying a shared chemical identity [2].

Scheele did not provide specific details for the synthesis of Scheele's green. The lack of details created challenges to obtain a single product. For this reason, several chemists have tried to reproduce the formulation of Scheele's green, not only with the objective to get a consistent product but also to be able to characterise the final product and give an exact formula [5, 9, 10, 11].

Historically, attempts to optimise the synthesis of Scheele's green have focused solely on adjusting the reaction temperature and the Cu:As ratios. This primarily involved comparing room temperature (cold reaction) with boiling solutions, exploring ratios of Cu:As such as 1:1, 1:2 and 3:2 [5, 6]. However, Saxena and Bhatnagar [11] introduced a crucial perspective by highlighting the role of pH in their investigation. Notably, they observed the formation of a single precipitate compound when titrating copper sulphate and sodium arsenite at a specific pH of 9.3, with a molar ratio of $\text{CuSO}_4:\text{NaAsO}_2$ of 1:2. Interestingly, like several other research groups, they noted that an excess of sodium arsenite led to hydrolysis and dissolution of the green product, a solubility challenge mitigated by maintaining low arsenite concentration and incorporating alcohol into the solutions. Their identified compound was designated with the formula CuAsO_2 .

Similarly, another research group delved into the production of copper arsenite across varying pH levels (pH 1–12). However, their oversight of the precipitation of arsenic trioxide at pH levels below 8 raises questions about the credibility of their findings [12]. While reporting good XRD spectra at lower pH, it's crucial to note that the resulting product corresponds to XRD peaks associated with arsenic trioxide crystals, indicating arsenic precipitation prior to the intended reaction. Furthermore, their product at pH 10 exhibited amorphous characteristics with no discernible XRD peaks.

In order to understand the synthesis of Scheele's green, this is, the reaction of arsenic (III) and copper ions from copper sulphate (the main form of copper used for the synthesis), it is essential to look at the behaviour of both ions in solution. From Fig. 1, it is evident that, at constant temperature and concentration, the dissociation of both ions depends on the pH of the solution. However, all but one of the published works regarding optimisation of the synthesis failed to recognise this fact. Below pH 8, arsenite exists as uncharged specie that readily precipitates at high concentration and is not likely to react with positively charged copper ions. On the other hand, at high pH above 10, copper tends to precipitate [13, 14] and arsenite exists as double and triple charge ions thus promoting the formation of more than one compound.

Analytical characterisation/identification of Cu-As green pigments

Various analytical methods can be employed for the identification of Cu-As pigments, encompassing techniques such as x-ray fluorescence (XRF), scanning electron microscopy with energy dispersive x-ray spectroscopy (EDX-SEM), polarized light microscopy, and chemical analyses, including atomic absorption (AAS),

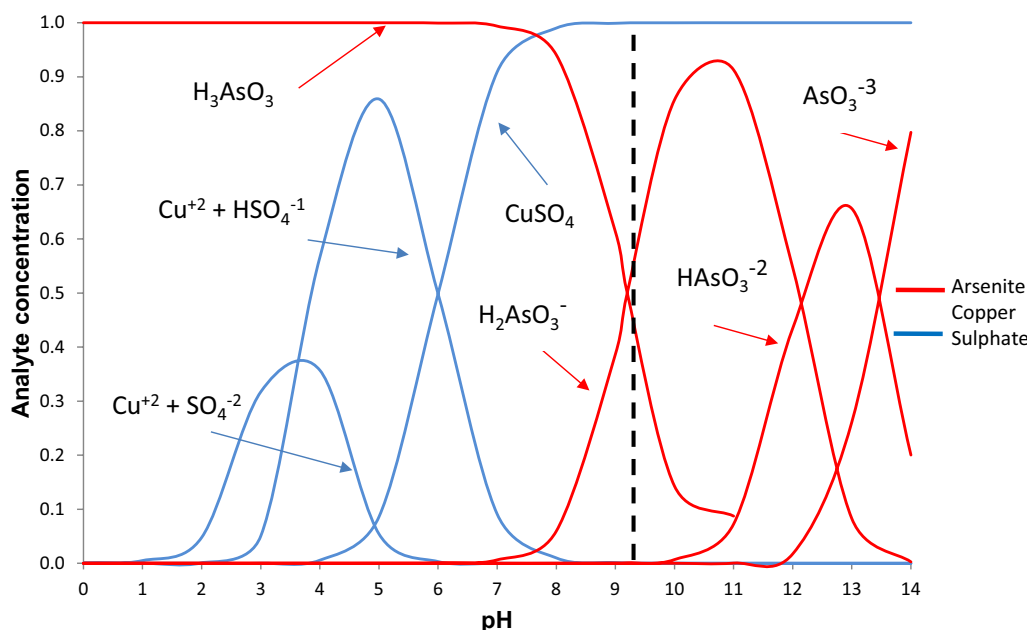


Fig. 1 Arsenite and copper sulphate speciation at different pH. Dissociation constants for copper from Davies et al. [14] and for arsenic, Jekel et al. [15]. Dashed line marks pH 9.3 as suggested by Saxena and Bhatnagar [11] to give a single product

inductively coupled plasma mass spectrometry (ICP-MS), and optical emission spectroscopy (ICP-OES). However, when it comes to distinguishing between Emerald and Scheele’s green, only Raman and infrared spectroscopy (FTIR), along with X-Ray diffraction (XRD), prove effective for this purpose [6]. Details for the Raman and FTIR vibrations for Emerald, Scheele’s green and Trippkeite are given in Table 1.

It’s important to highlight that only the Raman spectrum of both pigments has been documented with clear and well-defined positions, facilitating positive identification. In contrast, the reported FTIR spectrum for Scheele’s green exhibits noticeable differences, while the FTIR spectrum of Emerald green remains consistent, displaying well-defined vibrations of acetate groups. Consequently, the absence of these acetate vibrations could indirectly indicate the presence of Scheele’s green. This principle extends to XRD identification, where well-defined spectra characterise Emerald green, while amorphous Scheele’s green samples exhibit featureless spectra, serving as an indirect means of identification. For a more in-depth understanding of XRD band positions, readers are encouraged to consult the provided references [2].

It has also been reported that Emerald green can be identified by optical microscopy or SEM due to the spherical morphology of its particles [2]. Some researchers have also proposed the identification based on their Cu:As ratios [18] but both claims still need validation.

Table 1 Raman and FTIR bands for Emerald green, Scheele’s green and Trippkeite, from Bell, Clark, and Gibbs [16], Fiedler and Bayard [2] and Bahfenne et al. [17]

| Emerald green | | Scheele’s green | Trippkeite |
|---------------|------|-----------------|------------|
| Raman | FTIR | Raman | Raman |
| 122 | 641 | 135 | 134 |
| 154 | 689 | 201 | 203 |
| 175 | 765 | 234 | 235 |
| 217 | 819 | 274 | 285 |
| 242 | 1024 | 369 | 371 |
| 295 | 1420 | 444 | 421 |
| 324 | 1455 | 495 | 446 |
| 295 | 1560 | 536 | 496 |
| 324 | 3423 | 654 | 539 |
| 371 | | 780 | 657 |
| 430 | | | 780 |
| 491 | | | 810 |
| 539 | | | |
| 637 | | | |
| 686 | | | |
| 760 | | | |
| 836 | | | |
| 951 | | | |

Identification of Cu-As green pigments in practice

Adding to the characterisation complexity, it has been observed that the commonly produced forms of Scheele’s

green, yield indistinct and poor XRD spectra, indicating the amorphous nature of the product [2, 5, 6, 17]. It is well known that there is a correlation between sharp and well-defined XRD and Raman spectra [19, 20, 21, 22, 23]. This poses a challenge because it suggests that the amorphous Scheele's green product is unlikely to produce distinct Raman peaks. This observation challenges the findings of Bell, Clark, and Gibbs [16], who reported Raman spectra that would typically be associated with a crystalline form of the pigment. This contradiction raises questions about the nature of the Scheele's green product analysed in their study [16].

The theoretical complexities underlying the identification of Scheele's green compared to Emerald green in heritage objects could contribute to challenges of its identification in practice. This theoretical difficulty finds support in the limited instances of reported Scheele's green presence in heritage objects, totalling only 10 confirmed and documented occurrences (Table 2), with positive identification through Raman spectroscopy granted only to 5 of them. This stark contrast becomes evident when juxtaposed with the hundreds of confirmed and documented cases of Emerald green usage in cultural heritage objects [2].

Considering that Scheele's green was reported to be a very popular pigment and that continued to be available in manufacturers' catalogues until as late as 1898 [2], which is 120 years after its discovery, it seems perplexing that its presence is not as frequently reported when compared to Emerald green. Emerald green, banned at the start of the twentieth century, had about a century of usage after its discovery. Therefore, the apparent

imbalance in the occurrence of Scheele's green in heritage objects, in contrast to Emerald green, might stem from difficulties in accurately characterising Scheele's green rather than its infrequent use. However, this hypothesis requires experimental validation.

Degradation of As/Cu green pigments

It is well known that Emerald and Scheele's green tend to degrade with time. In published studies on the degradation of Emerald green, common assumptions prevail. It is generally described that Emerald green undergoes dissociation in acidic pH conditions, resulting in the generation of mobile arsenic trioxide and copper ions. This dissociation process is believed to contribute to the formation of brown or transparent layers in the affected objects [24, 25]. The migration of arsenic trioxide is considered to be a widespread phenomenon, extending to all layers of the studied surfaces. Additionally, a proposed oxidation of As(III) to a more mobile and water-soluble As(V) is suggested, and this transformation is thought to occur gradually, potentially mediated by bacterial activity due to its slow nature. Furthermore, the studies posit that As(V) reacts with lead, calcium and other ions present in the surrounding environment. This reaction is believed to lead to the formation of insoluble precipitates, contributing to the overall degradation process of Emerald green in heritage objects. Some studies even assume the transformation to happen at the exact same space in which the Emerald green spherulites are situated [26, 27, 28, 29, 30].

However, the degradation assumptions mentioned earlier overlook crucial observations made during the pigment manufacturing process. One notable observation is

Table 2 Reported use of Scheele's in heritage objects from previously published studies

| Date | Artist, country, title or description, location | Analysis and method of identification | Ref. |
|-----------|---|---|----------|
| 1805 | Joseph M. W. Turner, British, Oil sketch on panel, Guildford from the Banks of Wey, Tate gallery, London N02310 | EDX Scheele's green | [32, 33] |
| 1812–1814 | Dufour and Leroy, France, Le monuments de Paris, Paris | Raman Scheele's green | [34] |
| 1830 | Antonio Vighi, Russia, Historical house, Red living room plafond, St.-Petersburg | Raman Scheele's green/Emerald green | [35] |
| 1862 | Edouard Manet, French, Music in the Tuileries Gardens, National Gallery, London 3260 | EDX Scheele's green | [36] |
| 1866 | Edwin Landseer, British, Queen Victoria at Osborne Royal Collection, England | EDX Scheele's green | [2] |
| 1866 | Unknown, Germany, Roccoco stucco, Holzhausen, St Martin's Church, Upper Bavaria | FTIR Scheele's green | [6] |
| 1859–1884 | Henrique Pousao, 23 paintings from 1859–1884, collection of Museu Nacional Soares dosReis, Porto, Portugal | Raman Scheele's green/Emerald green | [37] |
| 1890–1920 | Spanish forger, England, 4 miniatures painted on vellum, V&A collection, | Raman Scheele's green/Emerald green | [38] |
| 19th C | Thang-ka, Nepal, Dr J. A. van der Hoeven private collection, Netherlands | No information given | [39] |
| 19th C | Scheele's Grun, Federal Austrian Authority for the protection of monuments, Austria | Raman, FTIR Scheele's green | [6] |
| 19th C | Unknown, Morocco, Dala'il al-Kayrat, private collection, Meknes and Fez | Raman Scheele's green/Emerald green | [40] |
| 19th C | Unknown, Shamanic painting of Bokgaedang Romance of three kingdoms, Korea, National Folk Museum of Korea | FTIR Scheele's green/Emerald green | [18] |
| 19th C | Fleury Richard, France, Powders on envelop, Musee des Beaux-Arts de Lyon | No information given, only XRF was done | [41] |

the presence of unreacted arsenic and copper, which persistently leach even after thorough washing of the product [5, 31]. Additionally, there is the potential for arsenic oxidation under prolonged boiling conditions, a requirement for some of the synthesis, leading to the generation of unreacted products. These unreacted arsenic species may contribute to arsenic migration during application, posing a risk of misinterpretation as degradation products.

Considering the gaps in knowledge regarding the optimisation of Scheele's green synthesis, challenges in its characterisation, limited instances of reported occurrences in heritage objects, and uncertainties surrounding its degradation, this study addresses these issues. It offers crucial details on the primary factor influencing Scheele's green synthesis, provides insights into its spectroscopic characterisation, explores its relationship with Emerald green, and challenges misconceptions regarding the stability and degradation of such pigments.

Aim

The aim of this study is to unravel the intricate factors influencing the synthesis of Scheele's green, investigate its relationship with Emerald green, and enhance the identification methods for these pigments in heritage objects. By addressing these critical gaps in knowledge, the research contributes valuable insights to inform cultural heritage preservation strategies associated with the use of these pigments.

Materials and methods

Synthesis

All formulations for the preparation of Scheele's and Emerald green have been previously documented and reviewed in existing literature. This study outlines briefly the steps undertaken for the synthesis of green Cu-As pigments, with references provided for detailed information:

Emerald Green (Gmelin, 1965, from [7]):

A. Dissolve 0.53 g of CuO in 1 M acetic acid with heating. After complete dissolution, add 1 g of As₂O₃. Boil and reflux for 24 h, wash the precipitate four times with distilled water, centrifuge and dry at 80 °C.

Trippkeite, from [8, 42]:

B. Mix 1.92 g of CuO and 2 g of As₂O₃ in a 1:1 molar ratio in 1 M acetic acid. Reflux for 48 h at 210 °C. Wash the precipitate three times with distilled water, centrifuge, and dry at 80 °C.

C. Mix 1.92 g of CuO and 2 g of As₂O₃ in a 1:1 molar ratio in water. Reflux for 48 h at 210 °C. Wash the precipitate three times with distilled water, centrifuge, and dry at 80 °C.

Scheele's Green:

D. From [5], original number formulation given (#):

D1. Method #11: Dissolve 4 g of sodium carbonate and 1 g of As₂O₃ in 5 mL of water. Separately, dissolve 3 g of CuSO₄·5H₂O in 20 mL of water. Boil both solutions and mix while hot. Allow to stand overnight, wash the precipitate with hot water four times, centrifuge and dry at 100 °C.

D2. Method #10 (Scheele's method): Dissolve 3.2 g of potassium carbonate in 3.2 mL of water, then add 1.1 g of As₂O₃ and boil until dissolved. Separately, boil 3.2 g of CuSO₄·5H₂O in 19.2 mL of water. Combine the two solutions with constant stirring. Centrifuge and wash the precipitate with distilled water four times.

D3. Modification of Method #11: Dissolve 1 g of sodium arsenite in 5 mL of water. Separately, dissolve 3 g of CuSO₄·5H₂O in 20 mL of water. Boil both solutions, mix while hot, and allow to stand overnight. Wash the precipitate with hot water deionised four times, centrifuge and dry at 100 °C.

E. From [43]: Dissolve 10 g of CuSO₄·5H₂O in 200 mL of water. Boil a mixture of 10 g of potassium carbonate and 3.25 g of As₂O₃ in 60 mL of water. Pour the arsenite solution slowly into the copper solution while hot. Wash with hot water four times, centrifuge and dry at 65 °C for 4 days.

F. From [12]: Dissolve 2 g of As₂O₃ in 20 mL of 1 M NaOH solution. Adjust the pH to 6 with H₂SO₄. The intended step (not executed due to precipitation): Add 5 g of CuSO₄·5H₂O [20 mmol] to the 20 mL solution of As₂O₃.

G. From [11]: Dissolve 2 g of sodium arsenite in 15 mL of water, then add 5 mL of ethanol. Adjust the pH to 9.3 with H₂SO₄. Dissolve 1.922 g of CuSO₄·5H₂O in 20 mL of water (pH 3.6). Mix the two solutions, centrifuge and decant the precipitate, repeat four times with cold water. Dry the precipitate at 80 °C overnight.

H. From [9]: Mix 8 g of potash with 1 g of As₂O₃ and dissolve in 183 mL of boiling water. Dilute the solution by adding 549 mL of water. Dissolve 9.14 g of CuSO₄·5H₂O in 183 mL of water. Mix the two solutions, centrifuge, and wash the precipitate four times.

Experimental pH was measured using a Jenway 3505 pH meter and calibrated using 4, 7 and 10 pH standards (Fisher Scientific). Theoretical pH calculation were made using the following dissociation constants for sodium carbonate, Ka1 = 4.5 × 10⁻⁷ and Ka2 = 4.7 × 10⁻¹¹, potassium carbonate Ka1 = 4.46 × 10⁻⁷ and Ka2 = 5.6 × 10⁻¹¹, palmitic and acetic acid, Ka = 1.75 × 10⁻⁵.

Analysis of historical samples

Table 3 shows a list of the historical and synthetic samples analysed in the present study. Historical samples were analysed with confocal Raman spectroscopy and

Table 3 Analysis of historical samples and synthetic samples for identification using Raman spectroscopy or free arsenic and copper as well as arsenic speciation

| Sample | Description | ID by Raman | Free As(III) ug/mg | Free As(V) ug/mg | % of As(V) | Free Cu ug/mg |
|--------|--|---------------------------------|--------------------|------------------|------------|---------------|
| S1 | Rowney & Co Emerald green oil paint tube, date unknown | Emerald green | 0.19 | ND | ND | 0.23 |
| S2 | Winsor & Newton Limited, Emerald green oil paint tube, post 1882 | Emerald green | 1.65 | ND | ND | 0.56 |
| S3 | Winsor & Newton Limited, Emerald green oil paint tube, post 1882 | Emerald/Scheele's green | 1.22 | ND | ND | 0.33 |
| S4 | George Rowney & Co Emerald green watercolour paint tube, date unknown | Emerald green | NA | NA | NA | NA |
| S5 | Newman's Emerald green watercolour cake, date unknown | Emerald green | 13.82 | 1.38 | 10.0 | 2.35 |
| S6 | Barnard's & son, Emerald green oil paint tube, date unknown | Emerald green | 0.36 | ND | ND | 0.08 |
| S7 | Winsor & newton, Emerald green Illuminating colours, date unknown | Emerald green/cobalt yellow | 23.68 | 6.23 | 26.3 | 2.24 |
| S8 | Acme quality paints Inc. Paris green poison, date unknown | Emerald/Scheele's green | 6.04 | 1.13 | 18.7 | 0.20 |
| S9 | Acme quality paints Inc. Paris green poison, date unknown | Emerald green | 12.84 | 0.72 | 5.6 | 0.21 |
| S10 | Bourgeois Aine, Emerald green Gouache colours, date unknown | Emerald green | 35.72 | 3.94 | 11.0 | 0.84 |
| S11 | Lefranc et Cie, Vert Veronese, oil paint tube, date unknown | Emerald green | NA | NA | NA | NA |
| S12 | Lefranc et Cie, Vert Veronese, oil paint tube, date unknown | Emerald green/Cerussite? | NA | NA | NA | NA |
| S13 | Lefranc et Cie, Vert Veronese, oil paint tube, date unknown | Emerald green | NA | NA | NA | NA |
| S14 | Lefranc et Cie, Vert Veronese, oil paint tube, date unknown | Emerald/Scheele's green | NA | NA | NA | NA |
| S15 | Bourgeois Aine, Unknown pigment, Gouache colours, date unknown | Emerald/Scheele's green | 13.48 | 17.65 | 131.0 | 5.75 |
| S16 | French 1858 papier peint (wallpaper) catalogue sample | Emerald/Scheele's green/unknown | NA | NA | NA | NA |
| S17 | Chipman Chemical company Inc, Paris green poison, date unknown | Emerald green | NA | NA | NA | NA |
| S18 | The poetical works of William Cowper, 1864, green spine | Emerald green | NA | NA | NA | NA |
| S19 | Die Technik der Olmalerei, 1911, W&N Emerald green sample paint | No Arsenic | NA | NA | NA | NA |
| S20 | A Descriptive Handbook of Modern Water-Colour Pigments, W&N, 1887 | Emerald green | NA | NA | NA | NA |
| S21 | Éléments de physiologie végétale et de botanique, 1815, 1er tableaux, plate 11 | Scheele's green | NA | NA | NA | NA |
| S22 | Velvotint Emerald powder colour, J. Barnard & Son | Emerald green | 9.49 | 1.07 | 11.3 | 0.58 |
| S23 | Vert de Scheele, oil paint, Richard Aine Paris | Calcite/Unknown | ND | ND | ND | 0.13 |
| A | Emerald green synthesis | Emerald green | 24.87 | ND | ND | 0.19 |
| B | Trippkeite Synthesis in 1M acetic acid | Emerald/Scheele's green | 34.62 | ND | ND | 0.30 |
| C | Trippkeite Synthesis in water | Scheele's green | 8.49 | ND | ND | 0.35 |
| D1 | Scheele's Synthesis | Unknown | 5.36 | 18.54 | 345.8 | 0.04 |
| D2 | Scheele's Synthesis | Unknown | 9.65 | 13.02 | 134.9 | 0.16 |
| D3 | Scheele's Synthesis | Unknown | 17.02 | 0.46 | 2.7 | 5.07 |
| E | Scheele's Synthesis | Unknown | 20.76 | 9.33 | 45.0 | 0.22 |
| G | Scheele's Synthesis | Scheele's green | 49.25 | 0.20 | 0.4 | 0.21 |
| H | Scheele's Synthesis | Unknown | 0.99 | 0.16 | 16.3 | 0.12 |

NA Not analysed, ND Not detected

compared to the accepted spectra of Emerald green and Scheele's green [16, 44]. All historical samples are part of a private collection in the UK, and appropriate permissions for their use have been secured.

Characterisation of samples SEM, EDX, Raman and FTIR SEM-EDX

Powder samples were analysed with a Phenom Pharos (Thermo Scientific) field emission gun scanning electron microscope (SEM) at high vacuum of 0.1 Pa and 15 kV acceleration voltage. Samples were mounted in aluminium studs using double-sided carbon adhesive tabs (Ted Pella), no coating was performed. Elemental composition was investigated through EDX with a silicon drift detector (SDD), 60 s analysis time per sample.

Raman

Confocal Raman microscopy was performed using a Labram Aramis (Horiba Scientific) using a 532 nm laser (1% power), a 50X objective, 600 l/mm grating, 50 μm pinhole, 3–60 s integration time and average of 10–60 spectra accumulations. Instrument was calibrated using a silicon wafer and automatic software correction (Labspec 6).

FTIR

Infrared analysis were performed with an IRAfinity-1S (Shimadzu) FTIR with diamond ATR, 60 scans, 4 cm^{-1} resolution and 400–4000 cm^{-1} range. Background signal was collected before each sample. Spectra was analysed using Omnic 7.0 (Thermo Scientific) software.

Elemental and speciation analysis

Elemental and speciation analysis of soluble fraction samples was performed as follows. Oil historical samples that had not dried up (indicating no exposure to air since production) were selected for extraction, alongside solid or powdered samples and dried, as-synthesized samples.

Samples were extracted by placing them in contact with HPLC mobile phase, then samples were immediately mixed by vortexing and centrifuged 15,000 rpm for 10 min to take a clear supernatant. The extraction protocol aimed to release only the free unreacted arsenic under very mild conditions and short contact time. The extraction was not intended to be optimal as the pigments are known to hydrolyse [5] at longer aqueous exposure times.

Elemental analysis (copper)

An aliquot of the same extracts used in the speciation analysis were diluted 20 times with deionised water and

analysed without further treatment. Total copper was analysed using an ICAP 6500 duo ICP-OES (Thermo Scientific) using a standard glass concentric nebuliser and a cyclonic spray chamber. The analysis was done in radial mode using the 324.754 nm copper emission wavelength, with an average of 3 readings per sample. Calibration curves were made using certified copper standards (1000 mg/L, Fisher Scientific).

Speciation of arsenic, HPLC-ICP-MS

All extracts were diluted 50 times with mobile phase before injection. Injection volume was 100 μL . Separation was achieved in a Hamilton PRP-X100 (10 μm , 250X4.1 mm) anion exchange column and isocratic elution, mobile phase 6.6 mM ammonium phosphate (sigma, 17842) and 6.6 mM ammonium nitrate (sigma 256064) adjusted to pH 6.3 with ammonium hydroxide. Flow rate was 1 mL/min [45]. The HPLC was connected to a tee piece and mixed with a 5 $\mu\text{g/L}$ solution of Rhenium as internal standard. Arsenic species were quantified in an iCAP RQ ICP-MS (Thermo Scientific) with kinetic energy discrimination KED using He as collision gas. The instrument was tuned daily and performance tests were done according to the manufacturer specification. Total run time was 12 min per sample. Stock solutions were prepared separately from sodium arsenate and arsenite, then mixed into calibration standards for analysis.

Results and discussion

Synthesis and characterisation

A notable gap in the existing literature emerges as the pH of starting solutions in Scheele's green synthesis experiments was unmentioned. This lack of information complicates predictions regarding the types of products formed in their experiments. However, leveraging their formulations allows for the calculation of theoretical pH, albeit with some uncertainties stemming from the purity of reagents during the eighteenth and nineteenth centuries. The following is a summary of the reactions and the theoretical or measured pH values:

- B Trippkeite, [8] theoretical pH 2.38 (considering 1 M acetic acid solution)
- D1, [5] #11, theoretical pH 12.38 (considering 4 g of sodium carbonate and 5 mL of water)
- D2, [5] # 10, theoretical pH 12.7 (considering 32 g potassium carbonate and 32 ml water)
- D3, [5] #11 modified, measured pH 12.3 (considering 1 g of sodium arsenite in 5 mL of water)
- E [43] theoretical pH 12.7 (considering 10 g of potassium carbonate and 3.25 g of As_2O_3 in 60 mL of water)

- G [11], measured pH 9.3 (considering 2 g of sodium arsenite in 15 mL of water then adjusted with H_2SO_4)
- H [9], measured pH 11.0 (considering 8 g of potash with 1 g of As_2O_3 in 183 mL of water)

From the data presented above, it can be observed that the synthesis of Scheele's green has historically been performed at pH above 11.

In this investigation, the synthesis of Emerald green (A) yielded a distinctive blue-green hue accompanied by a strong Raman signal (Additional file 1: Fig. 2SA and 4SA). Illustrated in Fig. 2A, the crystals exhibited morphology distinct from the reported spherulites in the literature. This deviation can be attributed to the deliberate implementation of constant stirring, aimed at ensuring a complete reaction. However, it is crucial to acknowledge that this approach compromises the typical spherulite morphology, as optimal spherulite formation occurs when the reaction is allowed to proceed undisturbed, as emphasised by prior research [7].

The synthesis of Trippkeite was performed as reported by Pertlik [8] and Kharbish [42]. This resulted in needle like crystals (Fig. 2B) that were mixed with other product as well as unreacted CuO. We confirmed the synthesis as the Raman spectra of single crystals matched the spectra of reported Trippkeite/Scheele's green (Fig. 3B2, top). The other product was consistent with the Raman spectra of Emerald green (Fig. 3B1, top), this was also confirmed by the bulk FTIR spectra that was dominated by the signal of Emerald green (Fig. 3B1 bottom). This was not expected (as this by-product was not reported by the original research), but is consistent with one of the methods to produce Emerald green, in which the addition of acetic acid (1 M) promotes the production of copper acetoarsenite. It was therefore decided to conduct the reaction only in water. The resulting material of such reaction is shown in Fig. 2C. It can be seen that smaller needle like crystals were formed and this time only a small fraction of unreacted CuO could be observed. The Raman spectra of Trippkeite synthesised in water matched the spectra of Trippkeite/Scheele's green (Fig. 3C top).

All the methods for the synthesis of Scheele's green but one, gave an unknown but similar Raman spectra. All spectra presented broad peaks at 288 and 845 cm^{-1} . One can observe the bands at 450 cm^{-1} in Fig. 3D2, E and G2 top, which could be attributed to the internal modes of the SO_4^{2-} ion and therefore belong to residual unreacted sulphate ions [46, 47]. The amorphous nature of such products can be observed in Fig. 2D, E and H, top. Sample D2 show the formation of small crystals, but it was still dominated by an amorphous solid (Fig. 2D2).

Herm [6], reported the Raman spectra of a sample labelled "Scheele' Grun", from the collection of the

Institute of Science and Technology in Art (ISTA) in Vienna. Such sample spectra, contains a broad band at 840 cm^{-1} in addition to not producing any peaks when using XRD. Herm [6] speculates that the sample is a "true Scheele's or mineral green" due to its FTIR spectra and relative featureless Raman spectra, despite not matching the generally accepted Raman spectra of Scheele's green.

Interestingly, only the synthesis performed at pH 9.3 gave a product with a strong Raman signal that matched the spectrum of "accepted" Scheele's green [16]. The SEM images confirmed the crystalline structure (Fig. 2G). Unfortunately, in their research, Saxena and Bhatnagar [11] did not record any spectra nor did any microscopy when they synthesised the original samples. It is important to note that such research and method was performed well after the pigment was banned and therefore a similar crystalline Scheele's green product is unlikely to be found in any historical sample.

The Infrared spectra of the bulk products can be observed in Fig. 3, bottom. The infrared spectra of Emerald green (A) (Fig. 3A bottom) was in very good agreement with the reference spectra in the CAMEO database [44].

As mentioned before, the synthesis of Trippkeite (B) included as a by-product copper acetoarsenite. The infrared spectrum in the bulk was dominated by the vibrations corresponding to Emerald green. The other by-product, unreacted CuO, does not have any observable vibrations in the infrared spectra (Additional file 1: sample C, Fig. 2SC2, FTIR spectra).

It's important to emphasise that the Raman and FTIR spectra of all synthesised products are displayed in Fig. 3. For detailed comparisons with other studies, certain spectra also featured in Figs. 4 and 5, employing different x-axis scales.

To the author's knowledge, the infrared spectrum of pure Trippkeite has not been reported in the literature before. Here, the FTIR spectrum is reported in Fig. 3C bottom and Fig. 4C, top, for the synthesis of Trippkeite (C) in water. Only two peaks can be observed at 473 and 732 cm^{-1} .

Infrared peaks for solid As_4O_6 have been reported at 480–482 cm^{-1} and very strong bands at 800–808 cm^{-1} , both bands are attributed to the As–O–As stretches [17]. Infrared studies on the $\text{As}_4\text{O}_6 \cdot \text{XH}_2\text{O}$ molecules have reported the presence of bands at 800 and 750 cm^{-1} . The 750 cm^{-1} band has been attributed to the hydrates and confirmed by the presence of bands at 3650, 3570 and 1600 cm^{-1} . None of such confirmation bands were found in the spectra of pure Trippkeite (Fig. 4C, top). Therefore, confirming that the As–O symmetric vibration observed normally at 800 cm^{-1} was shifted to 732 cm^{-1} in this crystal.

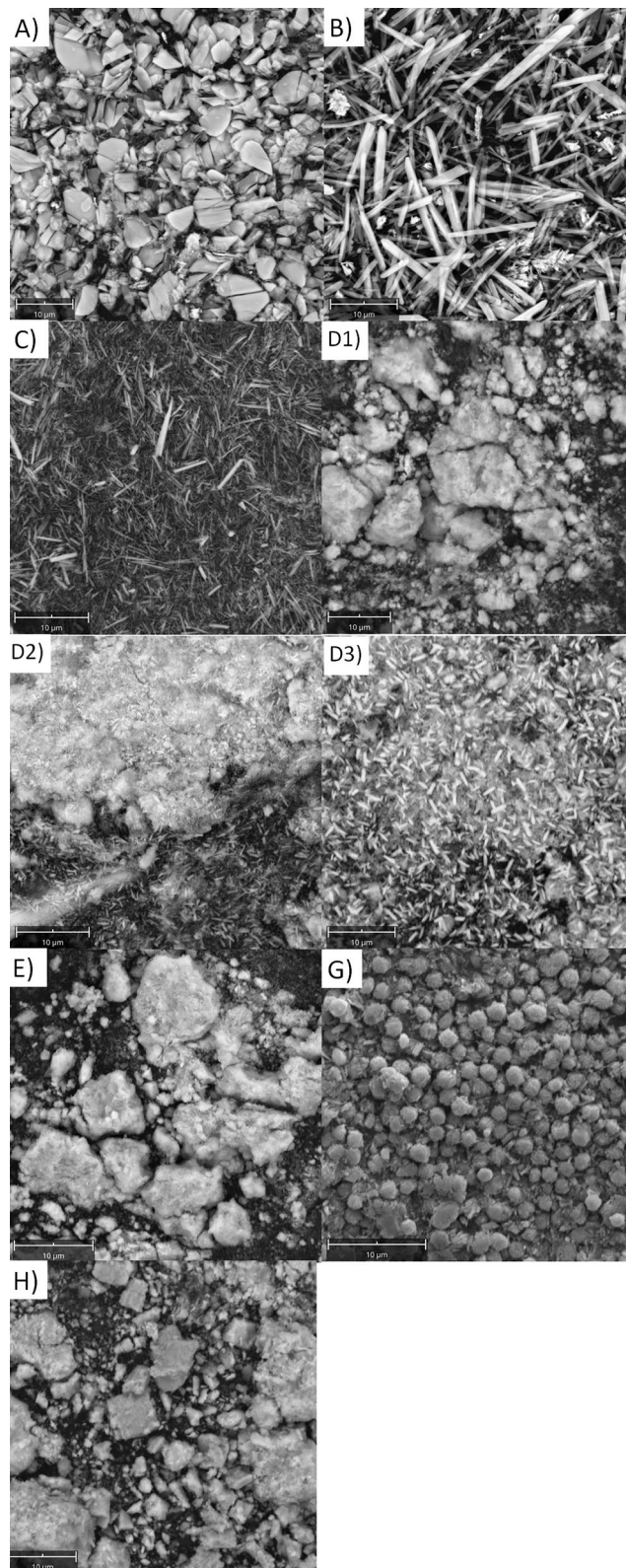


Fig. 2 FEG-SEM analysis of the synthesised products, reference to the method used is provided **A** Emerald Green, Gmelin (1965) from Scott [7], **B** Trippkeite, Pertlik [8] in 1M acetic acid, **C** Trippkeite, Pertlik [8] in water, **D1** Method #11, Sharples [5], **D2** Method #10, Sharples [5], **D3** Method #11 modified with sodium arsenite, Sharples [5], **E** Scheele's, Riffault et al. [43], **G** Scheele's, Saxena and Bhatnagar [11] and **H** Scheele's, Parker [9]

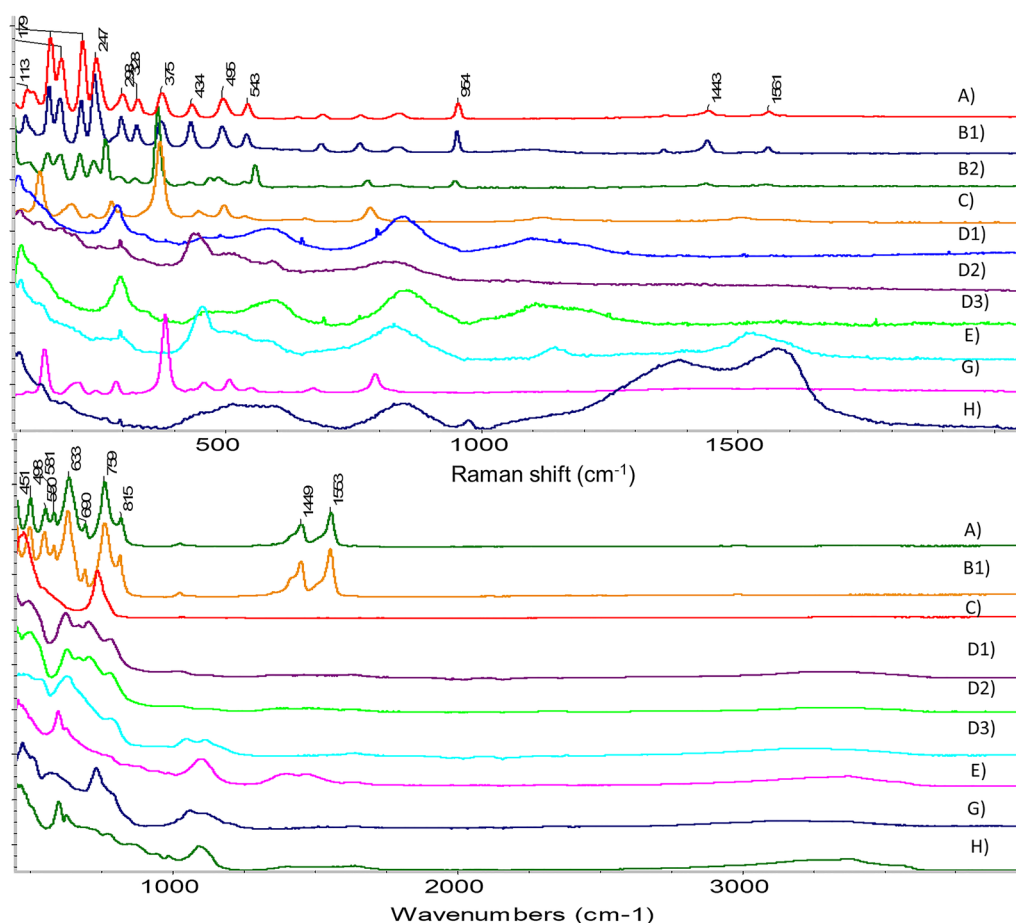


Fig. 3 Raman (top) and FTIR (bottom) spectra of the copper arsenite green pigments synthesised, **A** Emerald Green, Gmelin, 1965, from Scott [7], **B1** Trippkeite, particle 1, Pertlik [8] in 1M acetic acid, **B2** Trippkeite, particle 2, Pertlik [8] in 1M acetic acid, **C** Trippkeite, Pertlik [8] in water, **D1** Method #11, Sharples [5], **D2** Method #10, Sharples [5], **D3** Method #11 modified with sodium arsenite, Sharples [5], **E** Scheele's, Riffault et al. [43], **G** Scheele's, Saxena and Bhatnagar [11] and **H** Scheele's, Parker [9]. Y-axis for Raman has arbitrary units and absorbance for FTIR

As pointed before, there is limited Raman spectral evidence of Scheele's green in the literature. It has also been speculated that Trippkeite and Scheele's green could be the same product since they share identical Raman spectra [2, 6].

As seen in Fig. 4C and G (top), the synthesis of Scheele's green using Saxena and Bhatnagar [11] method yields, in addition to identical Raman spectra, very similar FTIR spectra to the synthesis of Trippkeite product. The main difference is the absorption at about 1100 cm^{-1} . This band could be attributed to unreacted copper sulphate, also illustrated in Fig. 4 (bottom). Even when Trippkeite and the pigment prepared using Saxena and Bhatnagar [11] method result in a different-looking product, as seen in Fig. 2B, C, and G (needle-like and spherulite crystals), the Raman spectra and FTIR spectra seem to indicate they are the same and have the same composition CuAs_2O_4 . The EDX analysis could not confirm such a formula; this is because the product may contain unreacted

copper and adsorbed arsenic, as explained in detail in the next section.

Fiedler and Bayard [2] observed distinct XRD patterns in two samples labelled as copper arsenite (presumed to be Scheele's green). For one sample (cupric arsenite from ICN Pharmaceuticals, 22 July 1983), the data matched that of the mineral Trippkeite, with a few extra lines. These additional lines constituted the primary features of the other sample (Freer Gallery of Art, E. W. Forbes Pigment Collection, Scheele's green). However, a recent analysis by Bahfnene [17] on Pertlik's original sample revealed that it consisted of only 65% Trippkeite, 20% CuO , 14% Cu_2O , and trace amounts of Olivenite and Cornubite. This emphasises that the Trippkeite standard used for comparison might have also contained impurities. Nonetheless, there is evidence suggesting that a product generated using a method distinct from that of Trippkeite, comprising small isolated crystals and

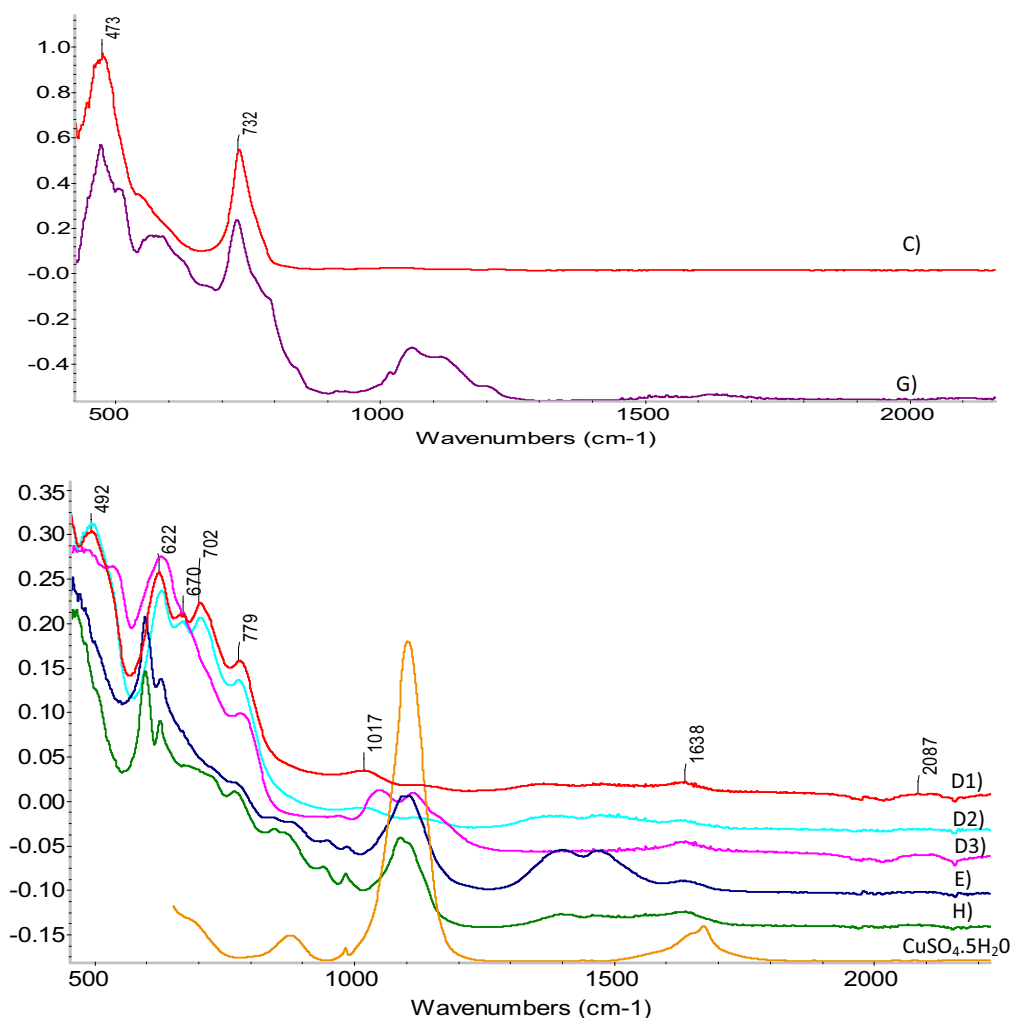


Fig. 4 Detailed comparisons of the FTIR spectra generated for synthesis **C** Trippkeite, Pertlik [8] in water and **G** Scheele's, Saxena and Bhatnagar [11], **D1** Method #11, Sharples [5], **D2** Method #10, Sharples [5], **D3** Method #11, modified with sodium arsenite, Sharples [5], **E** Scheele's, Riffault et al. [43], **H** Scheele's, Parker [9] and the spectra of pure copper sulphate for comparison (bottom), Y-axis has absorbance units

agglomerated multicrystalline nodules, exhibits identical XRD spectra to Trippkeite.

The details of the FTIR spectra for the rest of the synthesis methods for Scheele's green are given in Fig. 4 bottom. Synthesis D3, E and H also present a band at 1100 cm^{-1} that could be attributed to unreacted copper sulphate (Fig. 4D3, E and H, bottom). Synthesis D1, D2, D3, and H show a small peak at 779 cm^{-1} that can be attributed to hydrates since all show a small band at 1638 cm^{-1} as well as broad bands at about 3200 cm^{-1} (Fig. 4D1, D2, D3 bottom and Fig. 5 D1 and D3).

To the author's knowledge, only Herm [6], Oh, et al. [18, 48] and Fiedler and Bayard [2] have reported FTIR spectra of green pigments that contain copper

and arsenic and did not match the spectra of Emerald green. These samples correspond to:

- Scheele's' Grun, collection of the Institute of Science and Technology in Art (ISTA) in Vienna [6],
- Verde di Scheele, Opificio delle pietre dure [6]
- Scheele's green, W and J George and Becker sample [2]
- Scheele's green, Forbes Collection, Freer Gallery of Art [2]
- Shamanic paintings of Bokgaedang (shrine), solemn paintings (romance of three kingdoms) of Donggwanwangmyo, National Folk Museum of Korea samples 18,695 and 18,699 [18, 48]

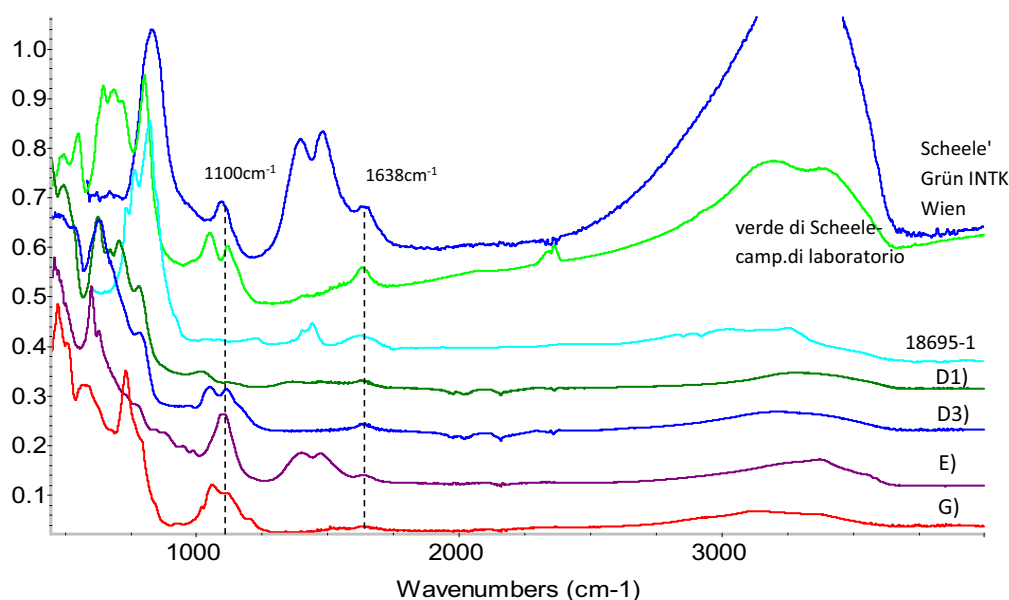


Fig. 5 comparison of FTIR spectra from published work and this study synthesis, Scheele' Grün INTK Wien, verde di Scheele-camp.di laboratorio, sample 18695-1, **D1** Method #11, Sharples [5], **D3** Method #11, modified with sodium arsenite, Sharples [5], **E** Scheele's, Riffault et al. [43], and **G** Scheele's Saxena and Bhatnagar [11]. Y-axis has absorbance units

The spectra reported in the literature were compared to the synthesis of samples D1, D3, E, and G in Fig. 5. Samples H and D2 were omitted to simplify the analysis because they have very similar spectra to E as D1 respectively. Fiedler and Bayard [2] point out the similarity of both the Forbes and W and J George and Becker samples. Both present bands near 1000–1100 cm^{-1} as well as bands at 810 cm^{-1} . As pointed before, the bands seen at 1100 cm^{-1} could be attributed to unreacted copper sulphate. In addition, all spectra present peaks at about 1638 cm^{-1} as well as broad peaks at 3200 cm^{-1} therefore suggesting hydrates (Fig. 5). It is crucial to note that such hydrated products may originate from unreacted hydrated copper sulphate rather than from the hydrated Cu-As pigment itself, as suggested in the original literature on Scheele's green synthesis [6].

Except for the product obtained using Saxena and Bhatnagar [11] method, all synthesised products and those reported in the literature (illustrated in Fig. 5), appear to consist of an amorphous material containing unreacted impurities. These impurities might have affected the elemental analysis conducted on such samples believed to be Scheele's green, as evidenced by the persistent variability in the calculated Cu:As ratio. Furthermore, it is noteworthy that the As-O symmetric vibration, typically observed around 800 cm^{-1} , cannot serve as a reliable identification marker, as not all products exhibit the same band, sometimes showing shifts to lower wavenumbers. Additionally, unreacted arsenic trioxide introduces peaks

at 805 and 652 cm^{-1} , potentially explaining the presence of the bands in some samples but not in others.

It is for the reasons indicated above that the determination of Scheele's green based solely on FTIR spectra is deemed impractical and inconclusive. The complex nature of its synthesis, in terms of historical recipes, demands a comprehensive analytical approach beyond FTIR spectroscopy for accurate and reliable identification. Multiple factors, such as the pigment's crystalline or amorphous form, its interaction with other compounds, and the potential presence of impurities, contribute to the limitations of relying solely on FTIR spectra for identification. To achieve a more robust and precise analysis, Raman spectroscopy still seems more accurate. However, a combination of complementary techniques, including Raman spectroscopy, elemental analysis, and microscopy, is recommended.

Analysis of historical samples

In a quest to understand the vibrant greens of historical samples, identification analysis was conducted using Raman spectroscopy, capturing the spectra of 23 samples from various sources, including oil paint tubes, water-based mediums, books and wallpaper (as detailed in Table 3). While the majority of these samples were labelled as Emerald green, Paris green, or vert Veronese (French terminology for Emerald green), a few presented intriguing characteristics.

Surprisingly, six samples were confirmed, using Raman spectroscopy, to contain Scheele's green, even though none were explicitly labelled as such. Intriguingly, five of these Scheele's green-containing samples also exhibited the presence of Emerald green as an admixture. This aligns with prior reports of the coexistence of Scheele's green and Emerald green in heritage objects (as reported in Table 2), suggesting an historical trend.

The phenomenon gains depth when considering 10 documented cases of Scheele's green in heritage objects; remarkably, half of them also showcased traces of Emerald green (or the other way around) as can be observed in Table 2. This study hypothesis revolves around the possibility that the synthesis process of Emerald green could have inadvertently produced small amounts of copper arsenite in the form of crystalline Scheele's green. This theory found support in the controlled synthesis of Trippkeite in 1 M acetic acid, where the presence of Emerald green was indeed confirmed (Table 3).

However, an alternative explanation cannot be dismissed. It raises the intriguing possibility that manufacturers, potentially sharing equipment or containers, inadvertently introduced traces of Scheele's green into batches of Emerald green, as this pigment replaced the original Cu-As based pigment. Yet, it is known that W&N in the UK, a prominent player since 1832 in which admixtures were found (Table 3), never sold Scheele's green, eliminating the possibility of contamination within their production processes [2].

Notably, this study alone reports more positive identifications of Scheele's green than have ever been reported in the literature, with six samples compared to the five reports found in existing literature (Table 2 and 3).

This dual revelation not only sheds light on the intricate historical interplay between Scheele's green and Emerald green but also underscores the complexity of synthesising and preserving these iconic pigments over time. In that regard some work has been written about the possible degradation causes for green Cu-As based pigments. Details of this are provided in the next section.

Degradation of Emerald green

In this investigation, the aim was to scrutinise the prevailing assumption that Emerald green undergoes dissociation in acidic pH conditions, leading to the release of mobile arsenic trioxide and copper ions, followed by subsequent oxidation to As(V). The primary goal was to assess whether free arsenic and copper exist in unused, undegraded historical pigment samples of Emerald green and Scheele's green. Moreover, the speciation of such free arsenic ions was studied. The summarised results are presented in Table 3.

It's essential to highlight that 100% aqueous-based solvent with minimal contact time were used to extract and prevent hydrolysis of the products. In addition, only samples that were sealed and not dried as well as showing no signs of colour degradation were studied. Notably, oil-based samples exhibited minimal migration of arsenic due to the immiscible nature of the solvent. However, all other samples, showed varying levels of migration of free As(III) and As(V). Copper migration was observed in all samples, but its concentration was lower than that of arsenic. Importantly, there was no correlation between copper and arsenic concentrations, ruling out hydrolysis of the sample itself.

The outcomes of this study revealed that all samples, with the exception of one (Vert de Scheele, S23), exhibited leaching of free As(III). The amount of free As(III) and As(V) showed variations among samples. The analysis indicated that up to 3.5% of the sample was present as free As(III), while up to 1.8% existed in the oxidised As(V) form. Notably, the percentage of As(V) in relation to total arsenic ranged from 6–131%, suggesting that certain samples contained a higher proportion of free As(V) than As(III). Particularly, sample S15 contained intact arsenic trioxide crystals on the pigment surface, visually depicted in Fig. 7A and corroborated by EDX elemental analysis and Raman (Additional file 1: Fig. 2S15C).

Historically, some methods of synthesis relied on prolonged boiling of the samples. Such boiling can lead to oxidation of arsenite. In this study's results, only the synthesis performed at low pH (A and B) and the synthesis of Trippkeite in pure water, showed no signs of oxidation as indicated by the lack of As(V) form (Table 3).

Keune et al. [24] suggest that arsenic migration occurs through the multilayer paint structure, leading to transparent or dark brown layers. The authors report no other source of arsenic and assume that arsenic migration must be due to degradation.

Their hypothesis involves the formation of arsenic trioxide, which dissolves, oxidises to arsenic pentoxide, reacts with lead, calcium, and other ions, and is deposited as insoluble arsenates. In a similar study by the same authors [25], they propose Emerald green degradation based on SEM images that show morphologically degraded particles. The distribution of arsenic in all paint sections, along with higher concentrations around iron and aluminium particles and in the varnish layer, is highlighted. Their attribution of bands to copper carboxylate (1598 and 1420 cm^{-1}) is questionable, as can be seen in Fig. 6, these bands are also observed in Emerald green due to the same acetate groups. The report of disintegrated particles lacks clarity on their existence, and the assumption of their dissolution raises questions about the role of manufacturing processes versus mechanical

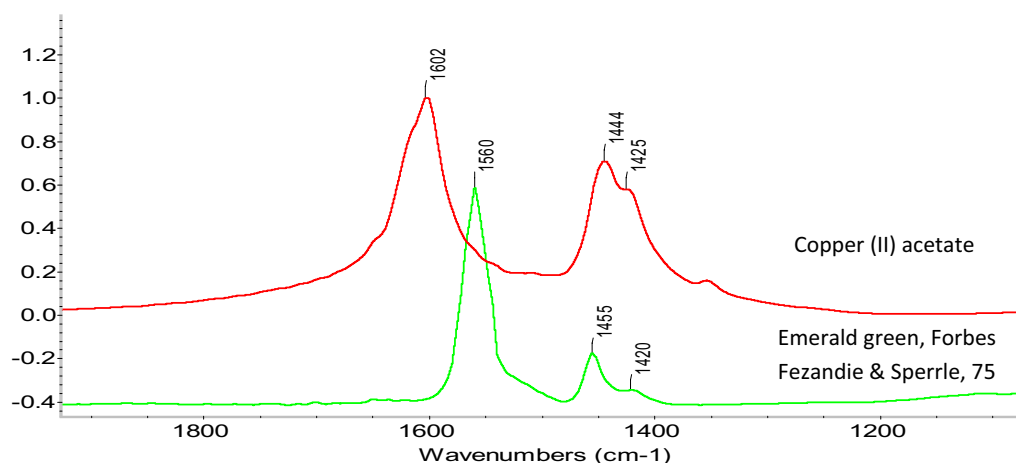


Fig. 6 Comparison of copper acetate and Emerald green, acetate group FTIR vibrations overlap. Y-axis has absorbance units

degradation. This because it is well known that the morphology of Emerald green particles depends on its manufacturing process [24, 25].

In addition, the conclusion that Emerald green reacts with free fatty acids to form copper soaps lacks sufficient evidence, especially considering their experiments at acidic pH levels (pH 2.53 and 2.06, calculated from the formulas provided) that are unlikely to represent any real conditions.

The consideration of free arsenic trioxide presence, without explaining the distribution of copper which does not seem to correlate with arsenic, raises doubts about the proposed reactions. The authors reference to arsenic trioxide's affinity to Fe and Al oxyhydroxides overlooks the pH dependence, as highlighted by experimental research where As(V) shows higher affinity to iron and aluminium at extended pH ranges [49].

Results from a different study, assert that Lammerite, a copper arsenate mineral, is a degradation product of Emerald green. The study on a rural Persian wall painting, employing Raman spectroscopy, suggests Lammerite as the primary pigment in the green layers. However, the claim of Emerald green's presence based on XRD spectra lacks support, as the reported peaks do not align with those attributed to emerald green (2θ value of 8.80°) [26, 50]. The authors speculate about Lammerite forming on the surface of Emerald green particles due to acid groups from the binding medium. Subsequently, they propose that oxidised arsenate, possibly accelerated by bacterial activity, recombines with copper ions to form Lammerite. This sequence of events contradicts natural occurrences of Lammerite, which typically form under extreme conditions of heat and pressure, such as in volcanic eruptions. Moreover, the formation of Lammerite requires high relative concentrations, a condition inconsistent

with the authors reported distribution of arsenic in all paint layers over time [51, 52, 53]. The study's conclusions appear uncertain, primarily due to the absence of the expected colour change indicative of a degraded product. For all the reasons explained above, Lammerite, as correctly identified by the authors, seems to have been used and applied as a pigment, rather than being a product of degradation.

In a more recent study, the presence of Cu and As pigments in polychrome paintings in China is reported. The Raman spectra exhibited broad bands at $825\text{--}835\text{ cm}^{-1}$, with Cu:As ratios ranging from 5:3 to 5:4 and a spherulite morphology. Based on these observations, the authors draw the conclusion that the pigment represents a degradation product of the originally used Emerald green. They argue that arsenic distributed in all the paint must have migrated from degraded Emerald green. However, their findings lack evidence supporting the existence of non-degraded Emerald green, and notably, there is a conspicuous absence of the expected colour change indicative of a degraded product [27].

In a separate investigation on a polychrome Dazu Rock carving statue in China, the authors confirm the presence of Mimetite and Cerussite. However, their interpretation exhibits inaccuracies, as they erroneously assert that Cerussite decomposes at low pH, whereas it is red lead that is known to be unstable in acidic conditions. Additionally, they assume that As(V) is more stable at low pH, when, in reality, at the same redox potential, As(III) is more stable under reduced pH conditions. The elemental maps presented in their study reveal a lack of correlation between Cu and As, with Cu distributed within particles and arsenic uniformly distributed across all layers. Furthermore, Na and Ca show no correlation with the presence of

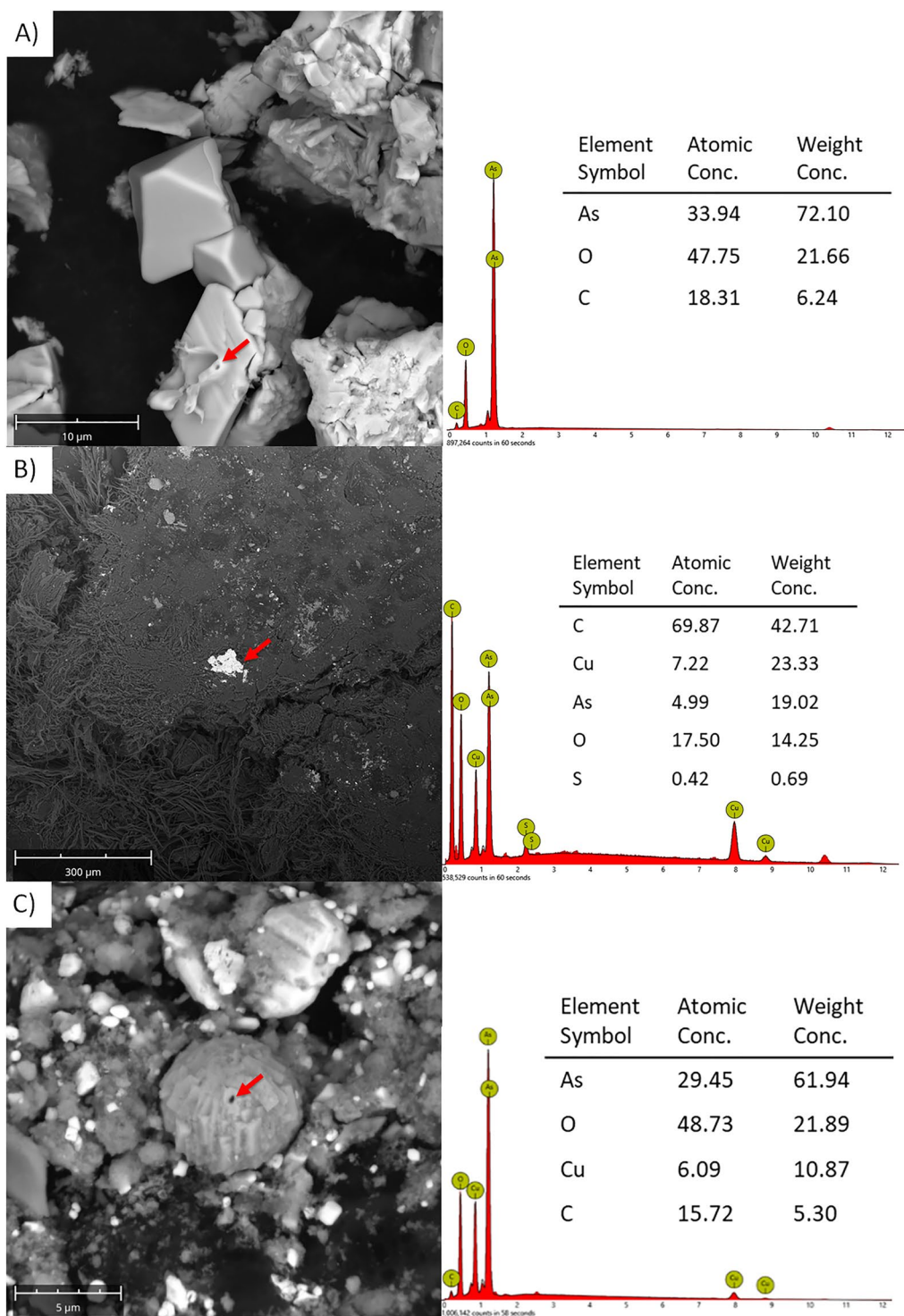


Fig. 7 SEM-EDX images of samples **A** S15, Bourgeois Aine, unknown pigment, Gouache, date unknown, **B** S18, The poetical works of William Cowper, 1864, green spine and **C** S21 *Éléments de physiologie végétale et de botanique*, 1815, 1er tableaux, plate 11, red arrow indicates the area for elemental analysis (right)

copper in particles. The authors attribute arsenic's presence in all layers to the degradation of Emerald green. A notable gap in their work is the absence of information regarding the method used to compare the colour of particles of Emerald green and Lavendulan [28].

In a study on the degradation and migration of arsenic in 19th-century Emerald green painted book bindings, the authors identify As(V) species and categorise them as degradation products, while all the As(III) found is labelled as non-degraded. They attribute the presence of copper hydroxide to unreacted production chemicals. However, the authors, facing challenges in providing a comprehensive explanation, assert that the apparently pristine green pigment has oxidised, and the oxidation product migrates away from the original Emerald green pigment. This raises questions about the interpretation of such degradation [29].

This study's analysis provides valuable insights into the possible degradation of Emerald and Scheele's green. It explains the migration of both forms As(III) and As(V). Such forms of free arsenic exist before any degradation happens and can, by definition, be mobilised into the layers of wet heritage objects from the moment of creation. The results provide an explanation for the apparent lack of colour degradation combined with arsenic migration observed by many studies. In the analysis of a book binding, specifically sample S18, a discoloration of the green pigment to a brown hue was observed (Additional file 1: Figure S18B). Upon further subsample analysis using SEM, it was identified that the degradation was more associated with the peeling/delamination of the green pigment, revealing the exposed brown cellulose material. This phenomenon is evident in the backscattered SEM image, where an intact particle of Emerald green (bright spot) is discerned against a backdrop of cellulose fibres (Fig. 7B).

Regarding the oxidation process from As(III) to As(V), it is crucial to consider that at neutral pH of 7, a redox potential of +60 mV is required to initiate oxidation, a kinetic process known to be slow [15]. This oxidation potential becomes even higher at low pH, reaching up to +400 mV, as indicated in the literature. Additionally, arsenite predominately exists as an uncharged ion at low and neutral pH. In contrast, arsenate undergoes ready ionisation and carries a negative charge at neutral pH. This characteristic results in a higher affinity for positively charged surfaces, such as Fe, Al, and Mn oxyhydroxides, making arsenate less mobile in the presence of iron-containing pigments but more mobile when not present.

It is essential to address a common misconception about this affinity. Arsenate and arsenite (at high pH) do not form chemical bonds with oxyhydroxides; instead,

they are adsorbed to the surface of these substances [54]. This adsorption is robust but reversible. Conversely, arsenate chemically reacts with free Ca^{+2} , Fe^{+3} , or Al^{+3} ions to create co-precipitates, adding a layer of complexity to the interactions involved. This clarification underscores the intricate dynamics of arsenic speciation in different environmental and pH conditions.

A subsample was taken from sample S21, from "Éléments de physiologie végétale et de botanique," book, dating back to 1815. Using SEM-EDX, it was verified the coexistence of arsenic and copper in the same location (Fig. 7C). In addition, Raman spectroscopy identified exclusively Scheele's green in this sample. To the author's knowledge, this is the first documented occurrence of Scheele's green in a book. Intriguingly, the spherulite-shaped particles resembled those obtained through the method proposed by Saxena and Bhatnagar [11] and the particles reported by Holakoei et al. [26]. This observation challenges a prevailing misconception associating spherulite morphology solely with Emerald green, emphasising the need for a re-evaluation of Emerald green identification based solely on particle morphology.

Conclusion

The evidence presented here indicates that the majority of historical recipes for Scheele's green resulted in amorphous materials, despite variations in Cu:As ratios and reaction temperature. Additionally, it was shown for the first time that, utilising the optimised pH of 9.3 was crucial for obtaining a crystalline product with an intense Raman signal. This Raman spectra aligns with the "accepted" spectra of Scheele's green.

The Raman spectra derived from amorphous Cu-As samples consistently exhibited broad bands at 288 and 845 cm^{-1} . Given the substantial evidence supporting the prevalence of amorphous Cu-As as the primary form of the green pigment, it is imperative to reassess these Raman spectra as representative of the "true" Scheele's green.

The widely accepted Raman spectra of Scheele's green potentially underrepresents the most commonly forms of copper arsenites, potentially explaining the limited reports of this pigment's use in heritage objects that stem from difficulties in accurately characterising it rather than its infrequent use. Here, it is proposed a modification for a dual representation of the pigment. The "common" form of Scheele's green with broad bands at 288 and 845 cm^{-1} and the "uncommon" or crystalline form as reported in the literature. The validity of a spectrum should not be determined merely by its visual appeal or ease of acquisition.

In this context, it is further illustrated that the crystalline variant of Scheele's green, not only exhibits

matching Raman spectra and reportedly shares identical XRD signals, but also displays nearly indistinguishable FTIR spectra. This strongly suggests an identical chemical composition to Trippkeite.

This study's evidence demonstrates that historically and recently produced pigments contain "free" copper, arsenite and arsenate ions. These ions are prone to migration into aqueous solutions or during application. This observation prompts to two critical considerations: firstly, potential miscalculations in Cu:As ratios based on pigment powders; and secondly, it provides crucial information for studying pigment degradation in heritage objects. This challenges the misconception that arsenic found distributed across all layers of heritage objects must originate from a degraded form of Emerald or Scheele's green. Instead, it offers a logical explanation for the apparent absence of colour degradation and provides tools for interpreting results when studying objects containing such green pigments.

The reported admixture of Emerald green and Scheele's finds clarification in this study, revealing that the synthesis of Emerald green may inadvertently lead to small amounts of Scheele's green. This highlights that caution should be taken when identifying such pigments with Raman spectroscopy. Additionally, evidence is presented for the first time of Scheele's green occurrence in a book. The particles found in the book have spherulite form thus challenging the identification of Emerald green based only on morphology.

The determination of Scheele's green relying only on FTIR spectra is considered impractical and inconclusive. The pigment's crystalline or amorphous form, interactions with other compounds, and potential impurities contribute to the limitations of using FTIR alone. For a more robust analysis, Raman spectroscopy remains a more accurate choice, but a combination of complementary techniques, including elemental analysis and microscopy, is recommended.

Supplementary Information

The online version contains supplementary material available at <https://doi.org/10.1186/s40494-024-01192-7>.

Additional file 1: Sample pictures, Raman spectroscopic identifications, (all y-axes have arbitrary units, name denotes sample type and identification), summary of the speciation and elemental analysis, inductively coupled plasma optical emission ICP-OES analysis and optical microscopy detailed images.

Acknowledgements

I would like to thank, Prof Christoph Herm and Dr. Oh Joonsuk for their kind help in providing reference spectra for comparison.

Author contributions

LP wrote the main manuscript, made substantial contributions to the conception or design of the work; or the acquisition, analysis, or interpretation of data;

or the creation of new software used in the work; drafted the work or revised it critically for important intellectual content; approved the version to be published; and agree to be accountable for all aspects of the work in ensuring that questions related to the accuracy or integrity of any part of the work are appropriately investigated and resolved.

Funding

No funding received.

Availability of data and materials

Data can be made available on request.

Declarations

Ethics approval and consent to participate

Not applicable.

Competing interests

The authors declare no competing interests. Declaration of generative AI and AI-assisted technologies in the writing process During the preparation of this work the author used ChatGPT/Classic in order to improve language and readability. After using this tool/service, the author reviewed and edited the content as needed and take full responsibility for the content of the publication.

Received: 14 December 2023 Accepted: 23 February 2024

Published online: 20 March 2024

References

- West JB. Carl Wilhelm Scheele, the discoverer of oxygen, and a very productive chemist. *Am J Physiol Lung Cell Mol Physiol.* 2014;307(11):L811–6.
- Fiedler I, Bayard. Emerald green and Scheele's green. In: Feller RL, editor. *Artists' pigments : a handbook of their history and characteristics.* Washington: National Gallery of Art; 2007.
- Lizun D, Kurkiewicz T, Szczupak B. Exploring Liu Kang's Paris practice (1929–1932): insight into painting materials and technique. *Heritage.* 2021;4:828–63.
- Jv L. Darstellung der unter dem Namen Wienergrün im Handel vorkommenden Malerfarbe. In: Buchner JA, Kastner KWG, editors. *Repertorium für die Pharmacie.* Nürnberg: Schrag; 1822. p. 446–57.
- Sharples SP. Scheele's Green, Its Composition as Usually Prepared, and Some Experiments upon Arsenite of Copper. *Proceedings of the American Academy of Arts and Sciences.* 1876; 12. p. 11–25 <https://doi.org/10.2307/25138431>.
- Herm C. Emerald Green versus Scheele's Green: Evidence and Occurrence. In *Acta Artis Academica 2020: The colour Theme : proceedings of the 7th Interdisciplinary ALMA Conference, 16th-18th october 2019 University Library Bratislava, Slovak Republic. Academy of Fine Arts in Prague, 2020.* 2019; 189–202 ISBN 9788088366140.
- Scott DA. *Copper and bronze in art: corrosion, colorants, conservation.* Los Angeles: Getty Trust Publications; 2002.
- Pertlik F. Verfeinerung der Kristallstruktur von synthetischem Trippkeit, CuAs₂O₄. *Tschermaks Min Petr Mitt.* 1975;22:221–217.
- Parker W. An improvement in the making or manufacturing of green paint. Patent. 1812;3:594.
- Schweizer F, Mühlethaler B. Einige grüne und blaue Kupferpigmente (Some green and blue copper pigments). *Farbe und Lack.* 1968;74:1159–73.
- Saxena RS, Bhatnagar CS. Electrometric studies on the composition of Scheele's Green (Product of mixing CuSO₄ and NaAsO₂). *Naturwissenschaften.* 1958;45(18):438.
- Xiao F, Zheng Y, Jian H, Li C, XU W, et al. Preparation of copper arsenite and its application in purification of copper electrolyte. *Trans Nonferrous Metals Socy China.* 2008;18(2):474–9.

13. Marani D, Patterson JW, Anderson PR. Alkaline precipitation and aging of Cu(II) in the presence of sulfate. *Water Res.* 1995;29(5):1317–26.
14. Davies WG, Otter RJ, Prue JE. The dissociation constant of copper sulphate in aqueous solution. *Discussions of the Faraday Society.* 1957; 24. p. 103–107 <https://doi.org/10.1039/DF9572400103>.
15. Jekel M, Amy GL. Chapter 11 Arsenic removal during drinking water treatment. In: Newcombe G, Dixon D, editors. *Interface science and technology.* Amsterdam: Elsevier; 2006. p. 193–206.
16. Bell IM, Clark RJH, Gibbs PJ. Raman spectroscopic library of natural and synthetic pigments (pre- ≈ 1850 AD). *Spectrochim Acta Part A Mol Biomol Spectrosc.* 1997;53(12):2159–79.
17. Bahfenne S, Frost RL. A review of the vibrational spectroscopic studies of arsenite, antimonite, and antimonate minerals. *Appl Spectrosc Rev.* 2010;45(2):101–29.
18. Oh JS, Choi JE, Choi TH. Study on the copper-arsenic green pigments used on shamanic paintings in the 19–20th century. *J Conserv Sci.* 2015;31(3):193–214.
19. Doumeng M, Berthet F, Marsan O, Delbé K, Denape, et al. A comparative study of the crystallinity of polyetheretherketone by using density, DSC, XRD, and Raman spectroscopy techniques. *Polymer Test.* 2021;93:106878.
20. Seehra MS, Narang V, Geddani UK, Stefaniak AB. Correlation between X-ray diffraction and Raman spectra of 16 commercial graphene-based materials and their resulting classification. *Carbon.* 2017;111:380–5.
21. Stacey P, Hall S, Stagg S, Clegg F, Sammon C. Raman spectroscopy and X-ray diffraction responses when measuring health-related micrometre and nanometre particle size fractions of crystalline quartz and the measurement of quartz in dust samples from the cutting and polishing of natural and artificial. *J Raman Spectrosc.* 2021;52:1095–107.
22. Charpentier C, Prodhomme P, Maurin I, Chaigneau M, Roca Cabarros IP. X-Ray diffraction and Raman spectroscopy for a better understanding of ZnO: Al growth process. *EPJ Photovolt.* 2011;2:25002.
23. Queiroz ALP, Kerins BM, Yadav J. Investigating microcrystalline cellulose crystallinity using Raman spectroscopy. *Cellulose.* 2021;28:8971–85.
24. Keune K, Boon JJ, Boitelle R, Shimadzu Y. Degradation of Emerald green in oil paint and its contribution to the rapid change in colour of the *Descente des vaches* (1834–1835) painted by Théodore Rousseau. *Stud Conserv.* 2013;58(3):199–210.
25. Keune K, Mass J, Mehta A. Analytical imaging studies of the migration of degraded orpiment, realgar, and emerald green pigments in historic paintings and related conservation issues. *Heritage Science.* 2016;4(10):1.
26. Holakooei P, Karimy AH, Nafisi G. Lammerite as a degradation product of emerald green: scientific studies on a rural persian wall painting. *Stud Conserv.* 2018;63(7):391–402.
27. Shen L, Wang C, Zhang J. Cu and As containing pigments in Zhejiang architecture polychrome paintings: a case study of degradation products of emerald green. *Herit Sci.* 2023;11(1):9.
28. Li Z, Wang L, Chen H. Degradation of emerald green: scientific studies on multi-polychrome Vairocana Statue in Dazu Rock Carvings, Chongqing. *China Heritage Science.* 2020. <https://doi.org/10.1186/s40494-020-00410-2>.
29. Vermeulen M, Webb SM, Russick S, McGeachy AC, Muratore K, Walton MS. Identification, transformations and mobility of hazardous arsenic-based pigments on 19th century bookbindings in accessible library collections. *J Hazard Mater.* 2023;454:131453.
30. Abotaleb TAA. DEGRADATION OF EMERALD GREEN PIGMENTS ON EASEL PAINTINGS. *PalArch's J Archaeol Egypt/Egyptol.* 2021;18(8):2062–72.
31. Riffault J, Vergnaud AD. *Nouveau manuel complet du peintre en bâtiments, du fabricant de couleurs, du doreur, du vernisseur, du vitrier et de l'argenteur.* Paris: Roret; 1843.
32. Townsend JH. *Turner's painting techniques.* London: Tate Gallery; 1993.
33. Townsend JH. The materials of J.M.W. Turner: pigments. *Stud Conserv.* 1993;38(4):231–54.
34. Castro K, Perez-Alonso M, Rodriguez-Laso MD, Madariaga JM. Pigment analysis of a wallpaper from early 19th century: Les Monuments the Paris. *J Raman Spectrosc.* 2004;35:704–9.
35. Petrova O, Pankin D, Povolotckaia A, Borisov E, Krivul'ko T, Kurganov N, et al. Pigment palette study of the XIX century plafond painting by Raman spectroscopy. *J Cult Herit.* 2019;37:233–7.
36. Bomford D, Kirby J, Leighton J, Roy A. *Art in the making: impressionism.* London: The national Gallery; 1990.
37. Correia AM, Clark RJ, Ribeiro MIM, Duarte MLTS. Pigment study by Raman microscopy of 23 paintings by the Portuguese artist Henrique Pousão (1859–1884). *J Raman Spectrosc.* 2007;38:1390–405.
38. Burgio L, Clark RJH, Hark RR. Spectroscopic investigation of modern pigments on purportedly medieval miniatures by the 'Spanish Forger'. *J Raman Spectrosc.* 2009;40(12):2031–6.
39. Mehra VR. Note on the Technique and Conservation of Some thangka Paintings. *Stud Conserv.* 1970;15(3):206–14.
40. El Bakkali A, Lamhasni T, Ait Lyazidi S, Haddad M, Rosi F, Miliani C, et al. Assessment of a multi-technical non-invasive approach for the typology of inks, dyes and pigments in two 19th century's ancient manuscripts of Morocco. *Vib Spectrosc.* 2014;74:47–56.
41. Carole D, Wicky E, Bensalah-Ledoux A, Paccoud S, Le Luyer C, Pillonnet A, et al. The pigments of the painter Fleury Richard (1777–1852), a model for multidisciplinary study. *Heritage.* 2022;5:1276–94.
42. Kharbush S. Raman spectra of minerals containing interconnected As(Sb) O₃ pyramids: trippkeite and schafarzikite. *J Geosci.* 2012;57(1):53–62.
43. Riffault JRD, Vergnaud AD, Toussaint GA. *A Practical Treatise on the Manufacture of Colors for Painting: Comprising the Origin, Definition, and Classification of Colors; the Treatment of the Raw Materials Etc.* In: François Malepeyre ed, Philadelphia, H.C. Baird; 1874.
44. Congress Lo. CAMEO: a free internet reference on Materials used in the production and conservation of historic and artistic works. 2008. <https://www.loc.gov/item/2021688168>. Accessed 18 Nov 2023.
45. Liu WJ, Wood BA, Raab A, McGrath SP, Zhao FJ, Feldmann J. Complexation of arsenite with phytochelatin reduces arsenite efflux and translocation from roots to shoots in Arabidopsis. *Plant Physiol.* 2010;152(4):2211–21.
46. Liu D, Ullman FG. Raman spectrum of CuSO₄ · 5H₂O single crystal. *J Raman Spectrosc.* 1991;22:525–8.
47. Fu X, Yang G, Sun J, Zhou J. Vibrational spectra of copper sulfate hydrates investigated with low-temperature raman spectroscopy and terahertz time domain spectroscopy. *J Phys Chem A.* 2012;116(27):7314–8.
48. Oh JS, Hwang MY, Yamato A, Arai K, Lee SR. Comparison of pigments and estimation of production period in old and new celestial charts folding screens. *J Conserv Sci.* 2020;36(5):351–67.
49. Lu P, Zhu C. Arsenic Eh–pH diagrams at 25°C and 1 bar. *Environ Earth Sci.* 2011;62:1673–83.
50. Ma Z, Wang L, Yan J, Zhou W, Pitthard V, Bayerova T, et al. Chromatographic, Microscopic, and Spectroscopic Characterization of a Wooden Architectural Painting from the Summer Palace, Beijing, China. *Anal Lett.* 2019;52(10):1670–80.
51. Poulsen SJ, Calvo C. Crystal structure of Cu₃(AsO₄)₂. *Can J Chem.* 1968;46(6):917.
52. Magalhães MCF, Pedrosa de Jesus JD, Williams PA. The Chemistry of Formation of Some Secondary Arsenate Minerals of Cu(II), Zn(II) and Pb(II). *Mineral Mag.* 1988;52(368):679–90.
53. Starova GL, Vergasova LP, Filatov SK. Lammerite-β, Cu₃(AsO₄)₂, a new mineral from fumaroles of the Great Fissure Tolbachik eruption, Kamchatka Peninsula. *Russia Geol Ore Deposits.* 2012;54:565–9.
54. Pantoja Munoz L, Jones H, Garelick H. The removal of arsenate from water using iron-modified diatomite (D-Fe): isotherm and column experiments. *Environ Sci Pollut Res.* 2014;21:495–506.

Publisher's Note

Springer Nature remains neutral with regard to jurisdictional claims in published maps and institutional affiliations.